Error Analysis and Study of Schuler Oscillations for Inertial Navigation Systems (INS)

A PROJECT REPORT SUBMITTED TO THE FACULTY
OF THE UNIVERSITY OF MINNESOTA
BY

Jyot R. Buch
Ph.D. Student in Department of Aerospace Engineering and Mechanics

IN PARTIAL FULFILLMENT OF THE REQUIREMENTS
FOR THE COURSE
NAVIGATION AND ATTITUDE DETERMINATION SYSTEMS
AEM 8442, FALL, 2018

December, 2018

Abstract

An Inertial Navigation System (INS) is a self-contained navigation technique in which measurements provided by accelerometers and gyroscopes are used to track the position, velocity and orientation of an object relative to a known starting point. Providing accurate initial conditions to the inertial navigator is one of the key challenge as any errors in actual navigation state and computed navigation state accumulates over time. However, due to the curvature of the earth acting as a feedback, most errors do not grow unboundedly but exhibits an oscillatory behavior which are referred to as *Schuler Oscillations*. This behavior is observed after ignoring the states which grow unboundedly and removing their influence from the dynamics. The initial condition error behavior for INS has been studied and MATLAB simulation results are discussed in this report.

Contents

Chapter 1

Introduction

An inertial navigation system (INS) is a navigation aid that uses a computer, motion sensors (accelerometers), rotation sensors (gyroscopes), and occasionally magnetic sensors (magnetometers) to continuously calculate by dead reckoning the position, the orientation, and the velocity (direction and speed of movement) of a moving object without the need for external references. It is used on vehicles such as ships, aircraft, submarines, guided missiles, and spacecraft for navigation purpose. Recent advances in the construction of microelectromechanical systems (MEMS) have made it possible to manufacture small and light inertial navigation systems. These advances have widened the range of possible applications such as mobile phones, robots, automobiles etc. Overall, INS technology has evolved gradually over time for aerospace, military and civilian applications. [1]

Even today, one of the key challenge for the pure inertial navigator is to initialize it with accurate initial conditions [4]. Here pure means without being aided by some other techniques such as GPS/GNSS. This is important for applications in GPS denied environment, urban environment where GPS suffers from multi-path errors or weapon systems such as Intercontinental Ballistic Missiles (ICBM) where the objective is to be self contained navigator and not rely on external signals. If initial conditions are not accurately representative of the true navigation state then this inaccuracy will grow over time as a result of continuous numerical integration [2]. But due to the curvature of the earth acting as a feedback, most errors do not grow unboundedly but instead results in the oscillation behavior which is known as *Schuler Oscillations* or *Schuler Feedback* [3].

1.1 Historical Background on Schuler Oscillations

Schuler oscillations are characteristic 84 minute cyclic responses of the correct navigation calculations in an INS to incorrect INS initialization and inertial sensor errors. The designation "Schuler Oscillations" for the 84 minute period error characteristics, is based on analogy to the behavior of an undamped pendulum having an 84 minute oscillation response to disturbances. Dr. Maximilian Schuler (a German scientist active during the early 1900's time period) reasoned that such a pendulum would remain vertical under horizontal acceleration of the suspension point. Thus, with such a pendulum, an accurate vertical reference could be established in a dynamic environment such as on a moving ship. His rationale for selecting the pendulum period was based on setting the pendulocity of the pendulum so that horizontal acceleration of the pivot over the earth surface produced angular acceleration that matched the equivalent angular acceleration of the pivot over the earth's curved surface. Dr. Schuler demonstrated analytically that the pendulum period to make this match would be 84 minutes, i.e., the same oscillation frequency as for INS horizontal errors. Without disturbances, a Schuler pendulum would remain vertical under horizontal pivot acceleration. If disturbed (e.g., by physically touching the pendulum), a Schuler pendulum would exhibit 84 minute oscillations (the reciprocal now known as the "Schuler frequency"). Similarly, for an INS without error, a gyro derived vertical reference frame within the INS would maintain a correct vertical orientation under system acceleration. However, if the INS contained errors, the gyro derived vertical reference would then exhibit 84 minute error oscillations from the vertical (as would the accompanying INS computed horizontal velocity and position outputs). Thus, in effect, implementation of an INS creates an artificial Schuler pendulum within the INS that exhibits the same error response behavior as a "real" Schuler pendulum. Schuler oscillations in an INS are caused by the effect of gravitational components (correctly modeled in the INS computer) that are perpendicular to the direction of motion [5].

1.2 Literature Review

The error behavior for the INS dynamical equations has been studied widely in the literature and presented with some detail. To motivate the importance further a brief

literature review on INS error behavior is included in what follows.

Propagations of INS errors dynamical equations in two-dimensional (Flat Earth) strapdown inertial navigation system exhibits unbounded error growth with time [5]. But since earth is not flat, but rather approximated by ellipsoid, the curvature of the earth plays a key role in providing dynamic feedback. This feedback results in oscillatory behavior and does not allow the navigation states to blow up with time. This phenomena was also shown in 40-years evolution of INS article [2]. Error and performance analysis of MEMS-based inertial sensors was presented in [8]. The influence of the stochastic variation of sensors was assessed and modeled by two different methods, namely Gauss-Markov (GM) and autoregressive (AR) models, with GPS signal blockage of different lengths. Sensor fusion for navigation of autonomous underwater vehicle using Kalman filtering was presented in [11] along with some detailed analysis on Schuler Oscillations. In [6] analysis of Inertial Navigation Systems (INS) was approached from a control theory point of view. Linear error models were presented and discussed, and their eigenvalues were computed in several special cases. Complex imaginary eigenvalue pairs resulted in the oscillatory behavior of dynamical response. It was shown that the exact expressions derived for the eigenvalues differ slightly from the commonly used expressions. The observability of INS during initial alignment and calibration at rest was analyzed. Few more technical reports/papers were referred during this work, as cited in the references, which discusses the Schuler oscillation behavior, but are not discussed here in this section.

Errors in INS navigation solutions are driven by initialization, computation and instrumentation errors. In this project, specifically the study of Schuler oscillation behavior due to initial condition error is presented. Several well known textbooks were referred during this work including ([13], [14], [15], [16], [17], [18]). Most of the work in this report is an attempt to reproduce the results shown in section 6.4 and 6.5 of [15] along with some references to [14] and [6].

1.3 Outline of Report

The organization of report is now provided.

- Chapter 2 discusses the technical approach that was used for conducting the study.

The linearized INS error dynamics from [15] or [16] are briefly stated for reference.

- Chapter 3 presents the results of MATLAB simulation for a stationary inertial navigator and discusses them in some detail.
- Chapter 4 provides the summary of this project and concludes the work.

Appendix A includes the MATLAB published code listings for further reference.

Chapter 2

Technical Approach

At least 3 methods are possible for analyzing the error performance of nonlinear system such as INS.

- First, the analyst can implement a nonlinear simulation of both the vehicle and navigation-system differential equations. The coupled differential equations are integrated for a given set of applied forced and the relevant state variables of the two systems are differenced to determine the navigation-system error. This approach requires high simulation rate and the (numeric) solution of nonlinear differential equations.

- Second, the analyst can linearize the navigation equations about a nominal trajectory of vehicle. The solution to the linearized navigation-system equations indicate the deviation of the navigation state from the actual vehicle state for a given trajectory. The given trajectory of the vehicle is needed to specify the F matrix completely. This trajectory is particularity simple for non-accelerating vehicles. This approach allows a much lower simulation rate since eigenvalues of the error system are quite small.

- Third, the analyst can linearize the navigation equations and perform a covariance analysis. This method has an advantage when generation of error statistics is the prime objective, of producing second order statistics for the error states from a single simulation run.

In this work, second method is used to illustrate the character of the solution of the INS error equations. These simulations are deterministic in nature, illustrating the error response due to specific assumed initial condition in the absence of any other error. The analysis is useful for motivating reduced order models, motivating certain INS calibration methods and generating an understanding of the system behavior. The presented analysis allows the prediction error growth in more general situations through the application of superposition and scaling, i.e. exploiting the linear properties.

To begin with, 9 state INS nonlinear equations corresponding to 3 position, 3 velocity and 3 attitude were obtained and linearized by hand following the linearizion procedure [20]. Significant discrepancy were found while comparing results with [15]. But, after referring to the latest edition of the same book [16], it was found that old edition had a typo and mismatch in the state vector order. In the interest of time, this linearizion steps are not included in this report. In what follows, we use the same notation as [16].

2.1 INS Linearized Equations

The linearize dynamic model for the nine primary error states is given by,

$$\delta\dot{\mathbf{x}}(t) = \mathbf{F}(t)\delta\mathbf{x}(t) + \mathbf{\Gamma q}$$

Where,

$$\mathbf{F} = \left[\begin{array}{ccc|ccc|ccc} 0 & 0 & \frac{\rho_E}{R_e} & \frac{1}{R_e} & 0 & 0 & 0 & 0 & 0 \\ \frac{-\rho_D}{\cos(\phi)} & 0 & \frac{-\rho_N}{R_e\cos(\phi)} & 0 & \frac{1}{R_e\cos(\phi)} & 0 & 0 & 0 & 0 \\ 0 & 0 & 0 & 0 & 0 & -1 & 0 & 0 & 0 \\ \hline F_{41} & 0 & F_{43} & k_D & 2\omega_D & -\rho_E & 0 & f_D & -f_E \\ F_{51} & 0 & F_{53} & F_{54} & F_{55} & F_{56} & -f_D & 0 & f_N \\ -2v_E\Omega_D & 0 & F_{63} & 2\rho_E & -2\omega_N & 0 & f_E & -f_N & 0 \\ \hline -\Omega_D & 0 & \frac{\rho_N}{R_e} & 0 & \frac{-1}{R_e} & 0 & 0 & \omega_D & -\omega_E \\ 0 & 0 & \frac{\rho_E}{R_e} & \frac{1}{R_e} & 0 & 0 & -\omega_D & 0 & \omega_N \\ F_{91} & 0 & \frac{\rho_D}{R_e} & 0 & \frac{\tan(\phi)}{R_e} & 0 & \omega_E & -\omega_N & 0 \end{array}\right],$$

and,

$$\mathbf{\Gamma} = \begin{bmatrix} \mathbf{0} & \mathbf{0} \\ -\hat{\mathbf{R}}_b^n & \mathbf{0} \\ \mathbf{0} & \hat{\mathbf{R}}_b^n \end{bmatrix} \text{ and } \mathbf{q} = \left[\left(\delta \mathbf{f}^b\right)^\top, \left(\delta \boldsymbol{\omega}_{ib}^b\right)^\top \right]^\top$$

following notations are used in above equations,

$\Omega_N = \omega_{ie}\cos(\phi)$	$F_{41} = -2\Omega_N v_e - \frac{\rho_N v_e}{\cos^2(\phi)}$
$\Omega_D = -\omega_{ie}\sin(\phi)$	$F_{43} = \rho_E k_D - \rho_N \rho_D$
$\rho_N = \frac{v_e}{R_e}$	$F_{51} = 2(\Omega_N v_n + \Omega_D v_d) + \frac{\rho_N v_n}{\cos(\phi)^2}$
$\rho_E = \frac{-v_n}{R_e}$	$F_{53} = -\rho_E \rho_D - k_D \rho_N$
$\rho_D = \frac{-v_e \tan(\phi)}{R_e}$	$F_{54} = -(\omega_D + \Omega_D)$
$\omega_N = \Omega_N + \rho_N$	$F_{55} = k_D - \rho_E \tan(\phi)$
$\omega_E = \rho_E$	$F_{56} = \omega_N + \Omega_N$
$\omega_D = \Omega_D + \rho_D$	$F_{63} = \rho_N^2 + \rho_E^2 - 2\frac{g}{R_e}$
$k_D = \frac{v_d}{R_e}$	$F_{91} = \Omega_N + \frac{\rho_N}{\cos(\phi)^2}$

State vector of interest is defined through, $\delta\mathbf{x} = [\delta\phi, \delta\lambda, \delta h, \delta v_N, \delta v_E, \delta v_D, \delta\epsilon_N, \delta\epsilon_E, \delta\epsilon_D]^T$ corresponding to the 3 position $[\phi, \lambda, h]^T$, 3 velocity $[v_N, v_E, v_D]^T$ and 3 attitude states $[\delta\epsilon_N, \delta\epsilon_E, \delta\epsilon_D]^T$, which represents a deviation from the actual state. Attitude states are positively defined small-angle rotations about the navigation-frame axis to align the navigation frame with the computed navigation-frame. ϵ_N and ϵ_E are referred to as tilt errors and ϵ_D is referred to as the heading, yaw or azimuth error. $\mathbf{q}$ vector represents the accelerometer (δf^b) and gyro ($\delta\omega^b$) errors which are representative of the forcing function for the linear system. In the forced analysis we use the following simplified convention to demonstrate the results, $\Gamma\mathbf{q} = [0, 0, 0, \delta f_N, \delta f_E, \delta f_D, \delta\omega_N^b, \delta\omega_E^b, \delta\omega_D^b]^T$. It is worth noticing that this is just a simplification for the simulations, in real scenario this forcing affects all the states. As shown in [16], the vertical channel position and velocity dynamics results in eigenvalues that have positive real part and thus exhibits an unstable behavior. For the simulation purpose we remove this 3^{rd} and 6^{th} states from the F matrix, and obtain the reduced order model of 7 states for analysis.

Chapter 3

Discussion of Results

The simulation for a stationary system (where actual states are at rest) with a set of initial condition error are included in this chapter and results are discussed in individual section. The simulation study is performed for a vehicle at rest on a sea level, located at 45^o north latitude (ϕ) for 40 hours. These results match with those shown in ([15],[16]).

3.1 Initial latitude error of 1 km

In Fig. 1 the error trajectory for the case of a 1-km initial latitude error is shown. The initial latitude error causes an error in the INS estimate of the north and the down earth rates; therefore azimuth and north tilt errors develop. The north tilt error directly causes east velocity error, which integrates into longitude error. The east velocity error is fed back into north tilt negatively, resulting in a low-amplitude Schuler Oscillation. The east velocity is fed back positively azimuth error, resulting in larger amplitude earth rate oscillations. The azimuth error also causes east tilt error and east tilt error and east velocity errors cause the north velocity error, which integrates in to latitude error. The north and the east tilt errors in Fig. 1 clearly show oscillations at Schuler frequency modulated at Foucault frequency. The azimuth, latitude and longitude errors are dominated by the earth rate oscillation. It is worth noticing the analytical expressions for Schuler and Foucault frequency as shown below. There is one more 24 h period oscillation corresponding to earth rate that can be observed from the results.

Fig.1 Stationary Error Response for 1 km initial latitude error

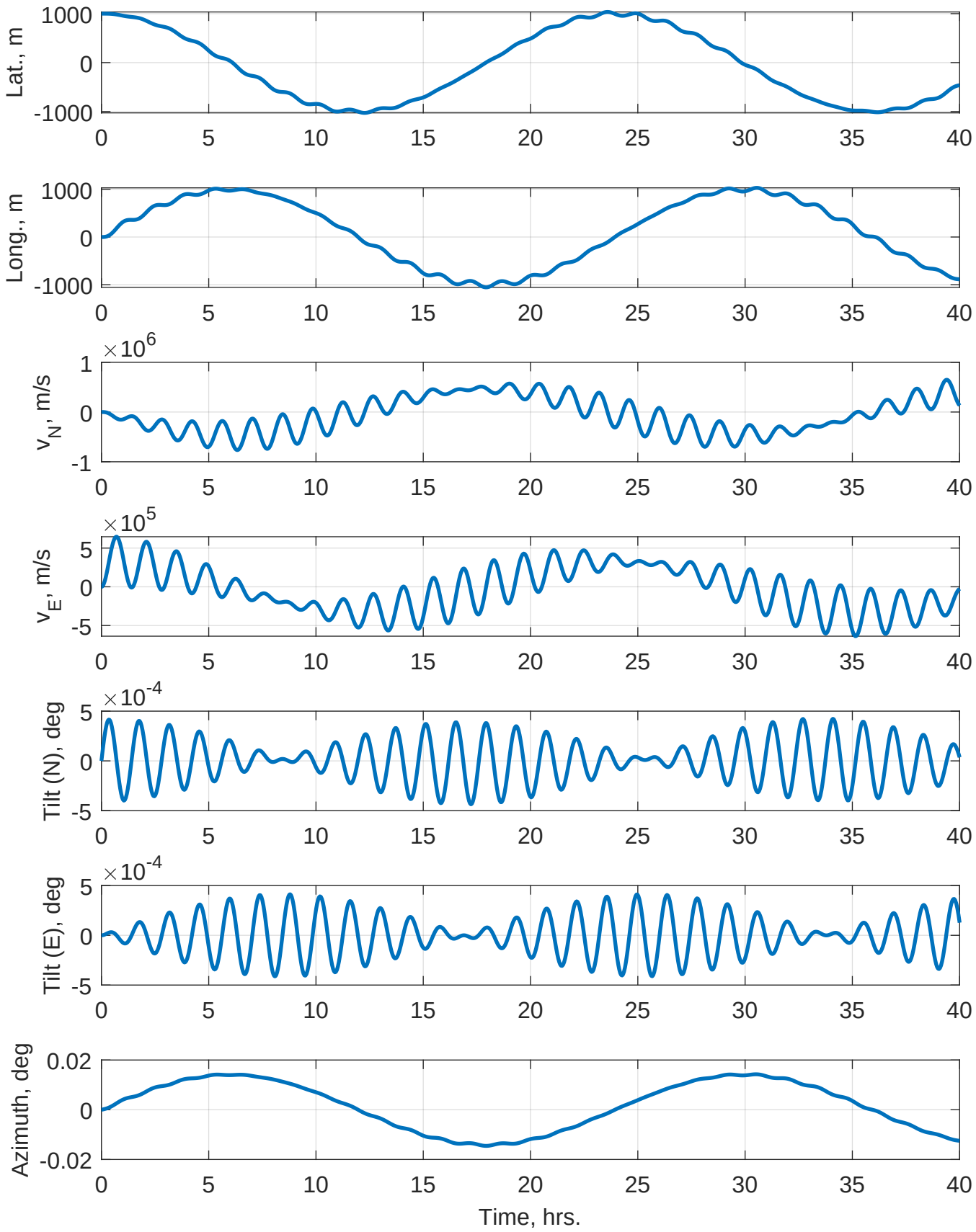

Schuler Frequency is given by $\omega_s = \sqrt{g/R}$, which results in Schuler period of 84.4 min oscillation. Foucault frequency is given by $\omega_f = \omega_e sin(\phi)$. At the latitude of the simulation, the period of the Foucault beat is 33.9 hrs. (see Appendix A)

3.2 Initial north velocity error of 1 m/s

In Fig. 2 the error trajectory for the case of a 1 m/s initial north velocity error is shown. The initial north velocity error directly causes east tilt error because of the error in the calculation of the earth relative navigation frame angular rate, east velocity error due to error in Coriolis compensation and latitude error by direct integration. All the five error states are dominated by the Foucault modulated Schuler oscillation. Because of the simulation occurring at latitude 45^o north the north tilt and the azimuth errors have equal order of magnitude.

3.3 Initial east velocity error of 1 m/s

Fig. 3 shows this case. The initial east velocity error directly causes azimuth and north tilt errors because of the error in the calculation of the earth-relative navigation frame angular rate (i.e. transport rate), north velocity error due to error in Coriolis compensation, and the longitude error by direct integration. All five states are dominated by Foucault modulated Schuler oscillations.

3.4 Initial 1 deg tilt about the north axis

Fig. 4 displays the error trajectory for the case of 1^o initial tilt about the north axis. The north tilt error directly causes error in the gravity and earth rate compensation, which results in east tilt and east velocity errors. The north and the east tilt plots show the Foucault modulated Schuler oscillation. The latitude, longitude, and azimuth errors are the superposition of earth rate oscillations and Foucault modulated Schuler oscillation.

3.5 Initial 1 deg tilt about the east axis

Fig. 5 displays the error trajectory for the case of a 1^o initial tilt about the east axis. The east tilt error directly causes error in the gravity and earth rate compensation, which results in azimuth, north tilt and north velocity errors.

3.6 Initial 1 deg azimuth error

In Fig. 6 the error trajectory for the case of a 1^o initial azimuth error is displayed. The initial azimuth error causes only east tilt error. It can be observed that nonzero value of the north velocity error integrates into significant latitude error, which ultimately causes the azimuth error to decrease from its maximum value and exhibit earth-rate dominated oscillations. The physical cause of the east tilt error is error in the earth rate calculations.

3.7 Initial constant gyroscope bias and accelerometer bias

Fig. 7, 8, and 9 shows the response of constant uncompensated north, east and azimuth gyro bias of $0.015^o/h$ respectively. Fig. 10, 11 includes the simulation results for 0.1 m/s^2 of initial north and east accelerometer bias error respectively, which results in very large velocity drift. In this work, as stated before we assumed that accelerometer bias error show up only in velocity dynamics (which is not a practical situation, as this biases and errors show up in all the states of interest), but this entirely depends on sensor model and characteristics. For simplicity of analysis constant biases were chosen. Reference [16] discusses the effect of gyroscope bias and accelerometer bias in some detail with analytical equations representing solutions of linear differential equations. Some numerical mismatch in these results are expected as the sensor error models used in this work was not exactly similar to those used in [16] but were rather close to ones that are used in [6].

Fig.2 Stationary Error Response for 1 m/s initial north velocity error

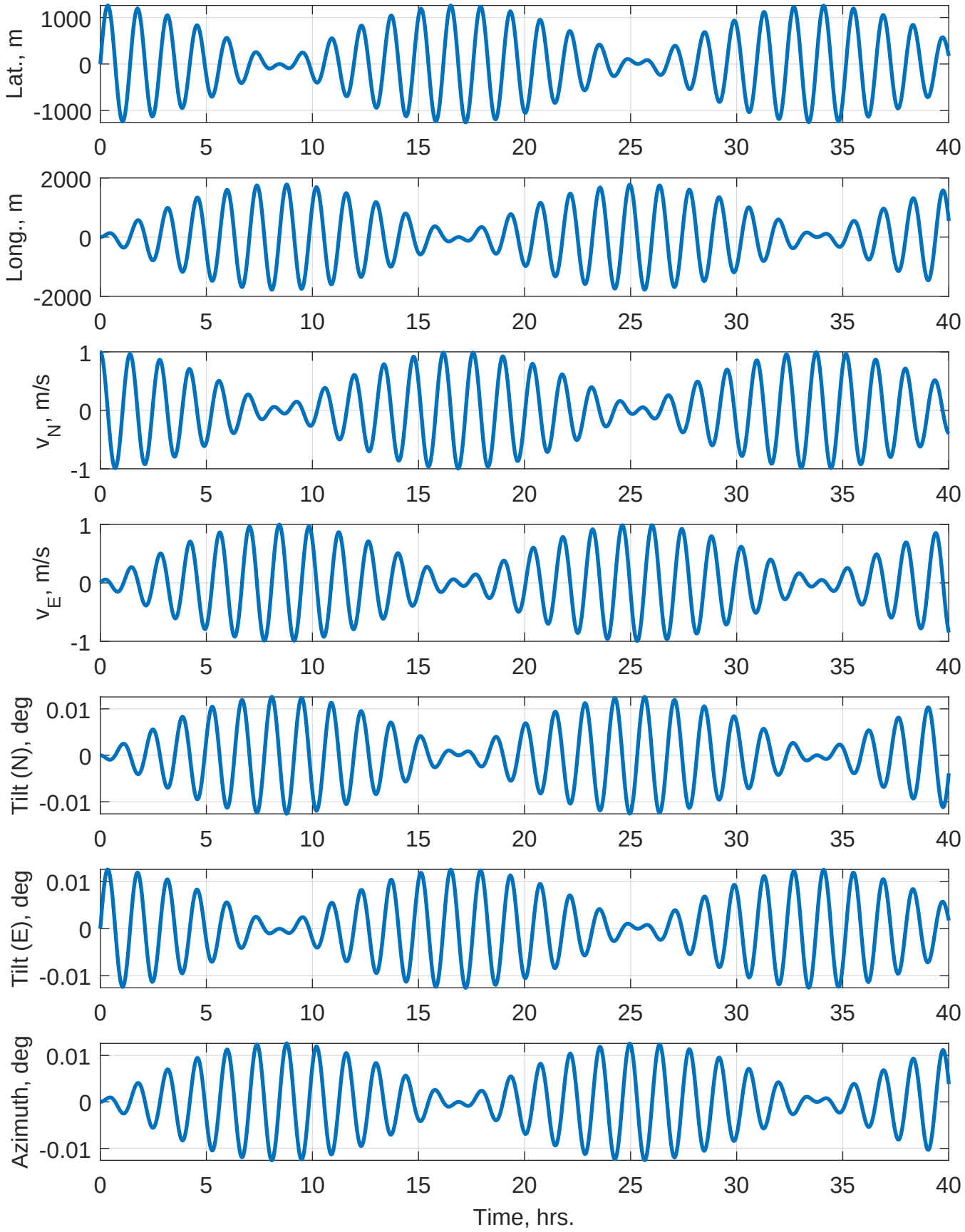

Fig.3 Stationary Error Response for 1 m/s initial east velocity error

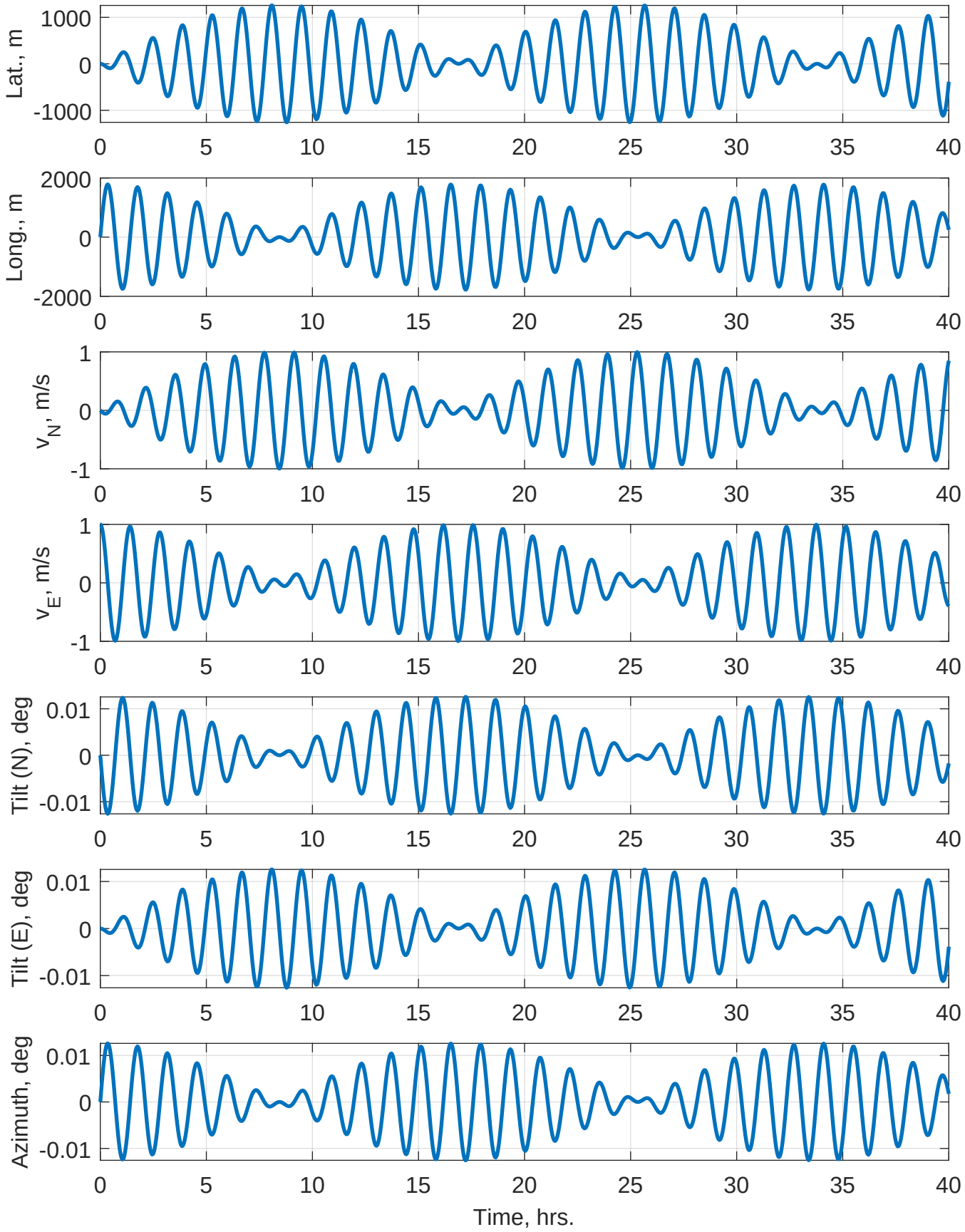

Fig.4 Stationary Error Response for 1^{o} initial north tilt error

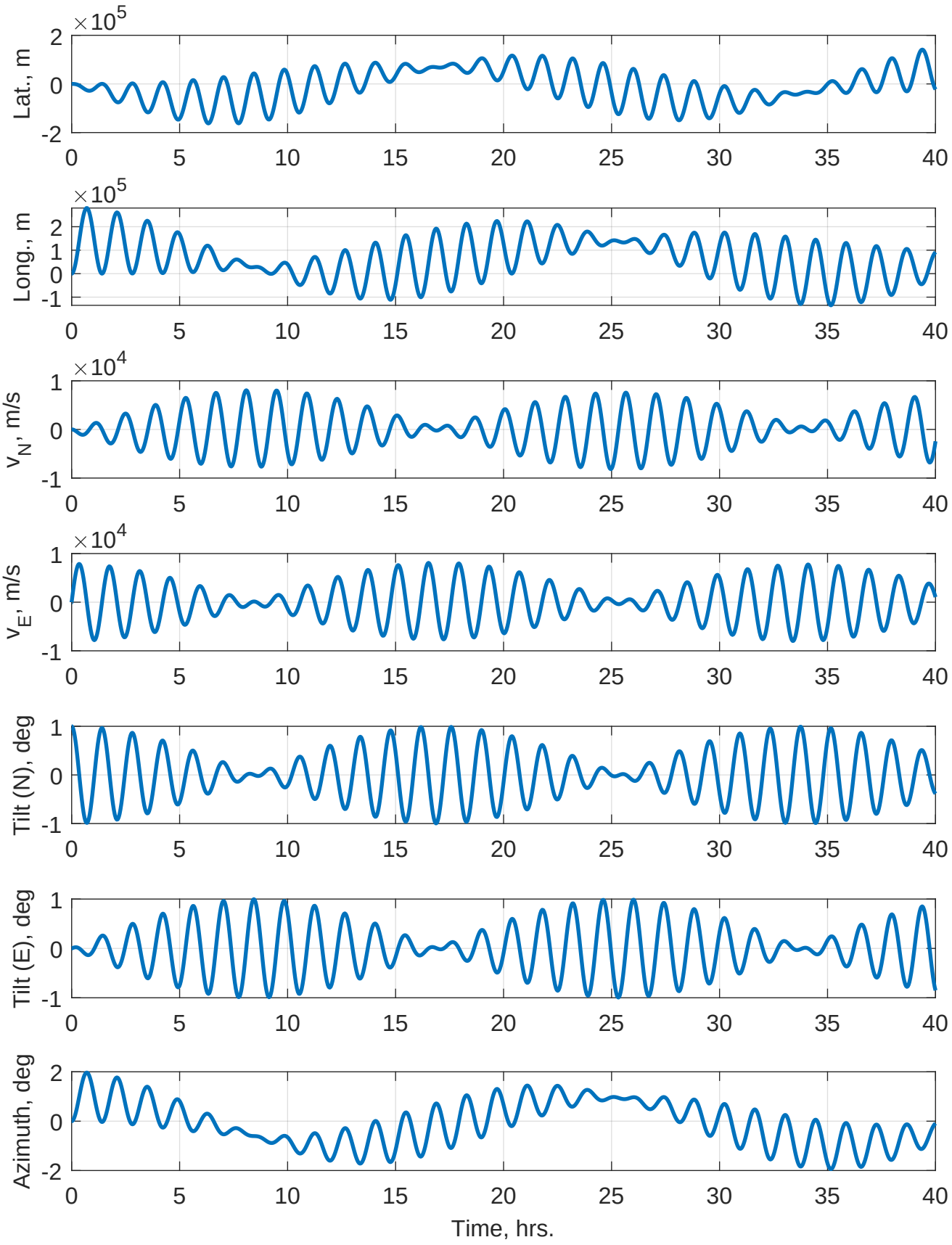

Fig.5 Stationary Error Response for 1^{o} initial east tilt error

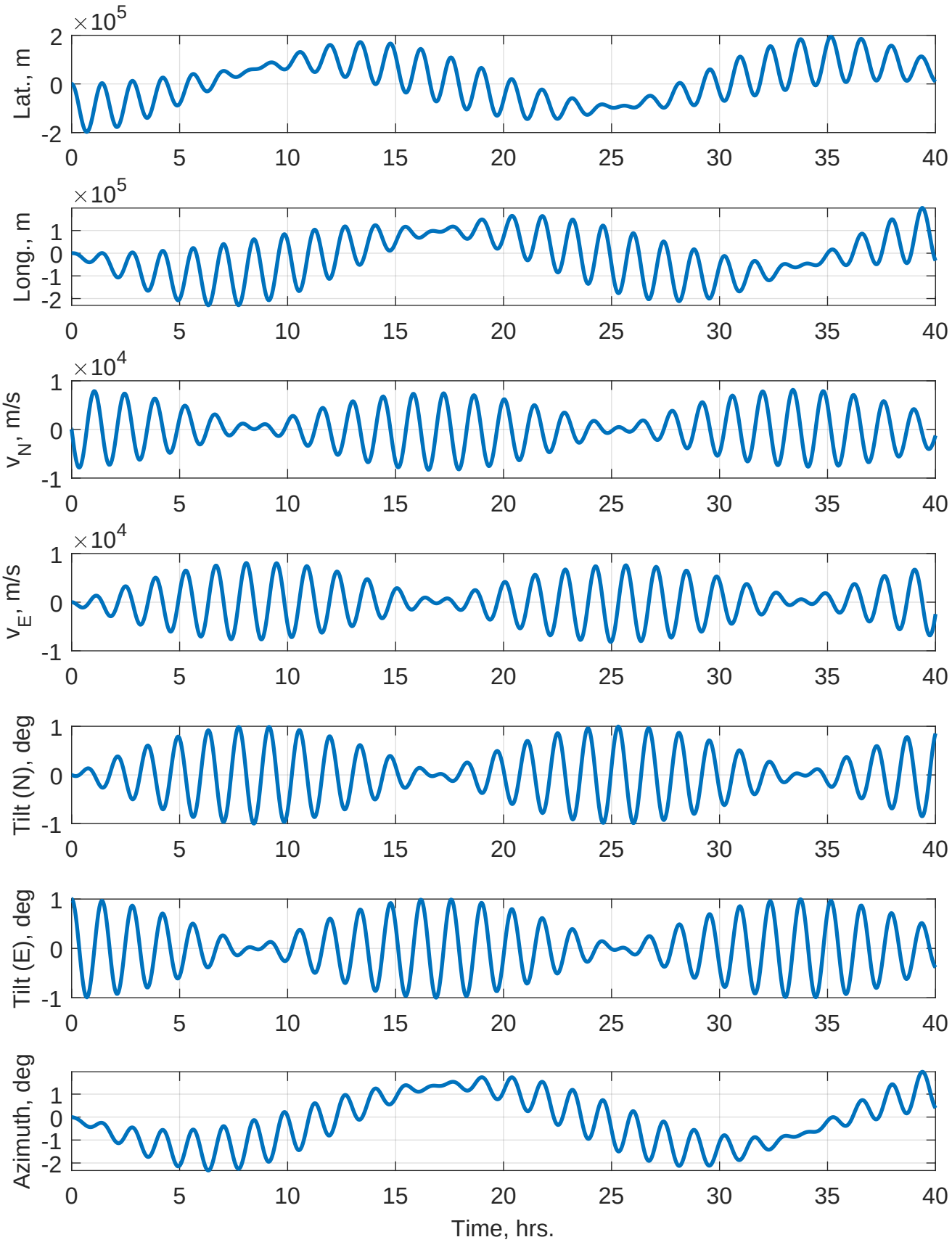

Fig.6 Stationary Error Response for 1^{o} initial azimuth tilt error

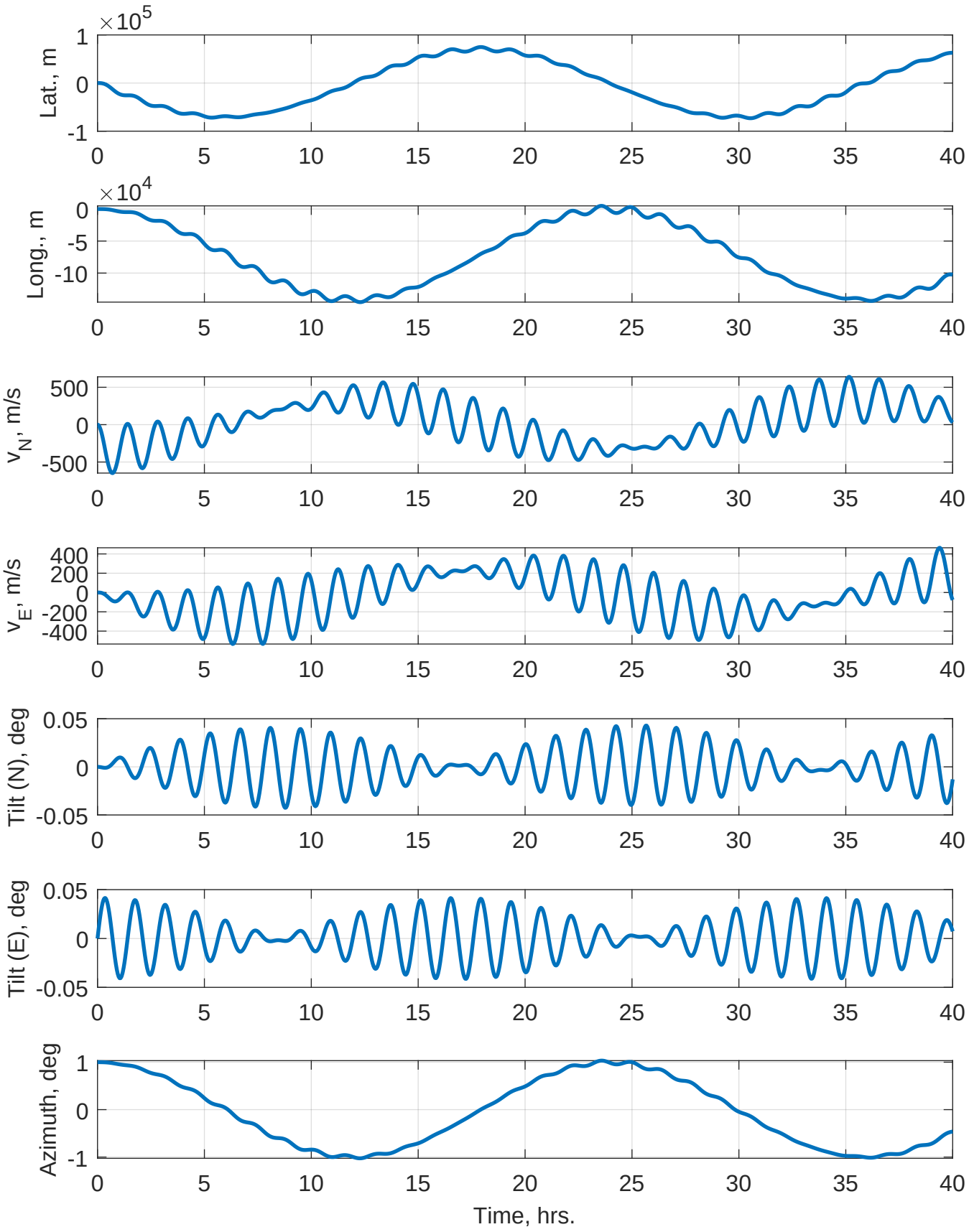

Fig.7 Stationary Force Response for 0.015^{o}/h initial north gyro bias

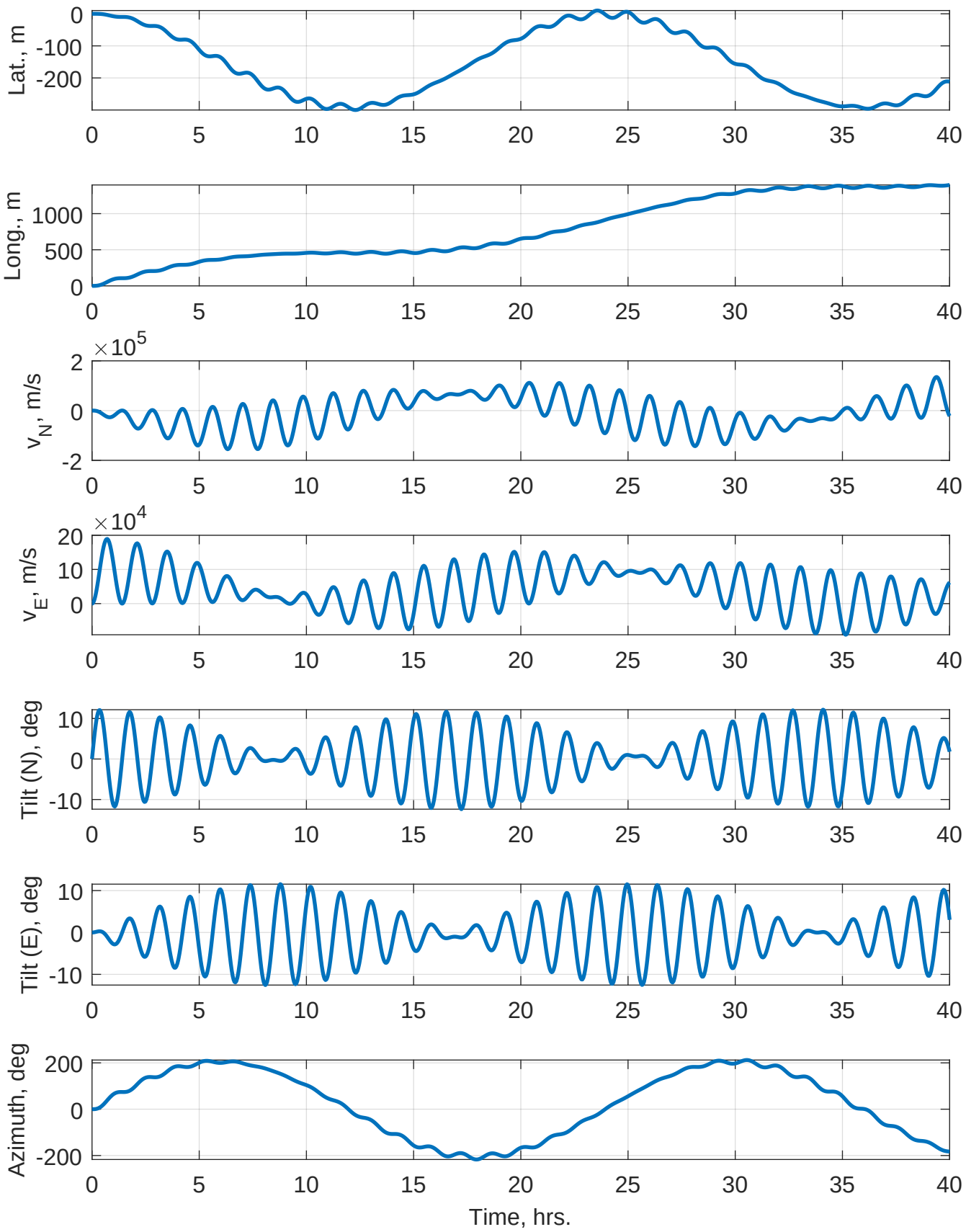

Fig.8 Stationary Force Response for 0.015^{o}/h initial east gyro bias

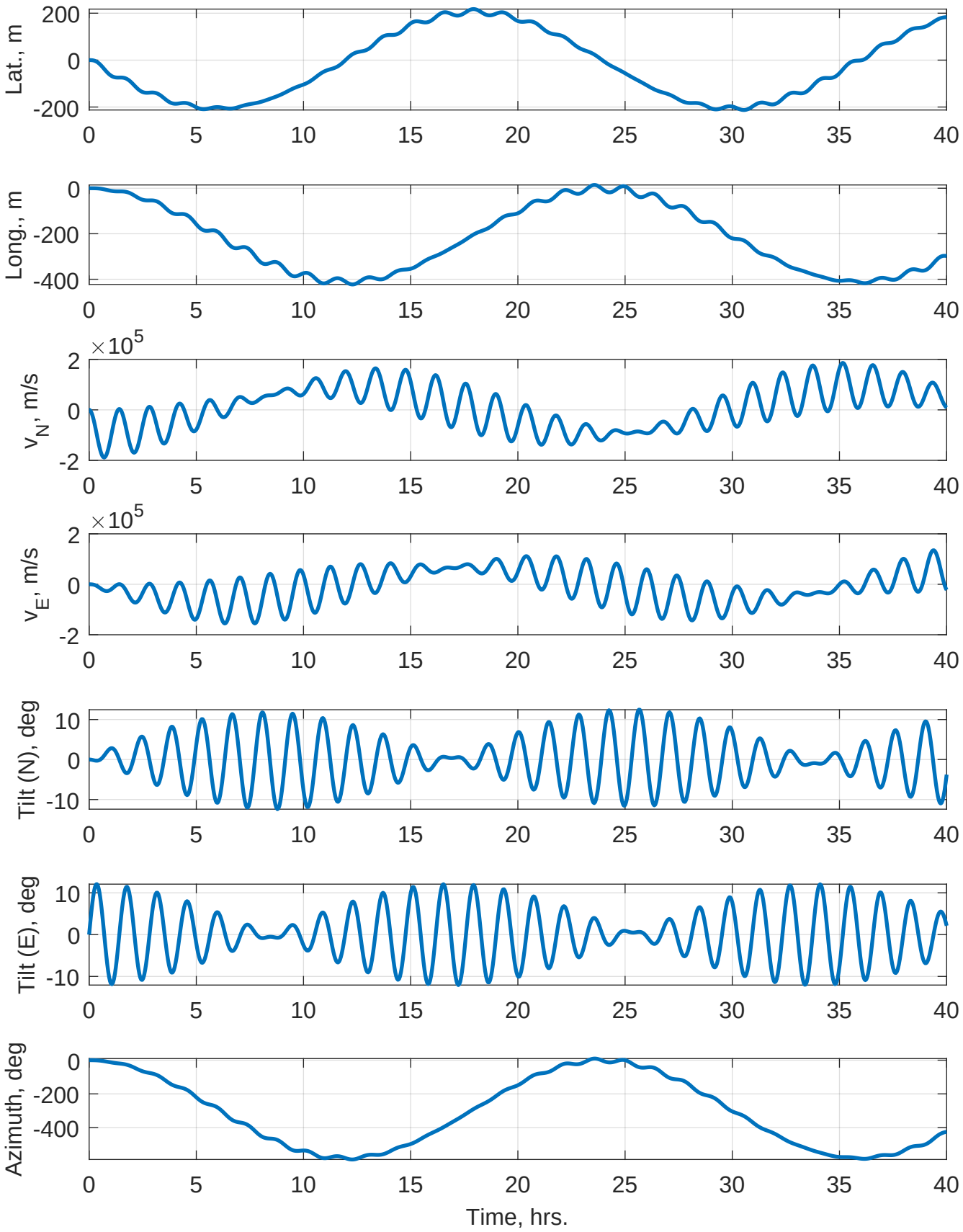

Fig.9 Stationary Force Response for 0.015^{o}/h initial azimuth gyro bias

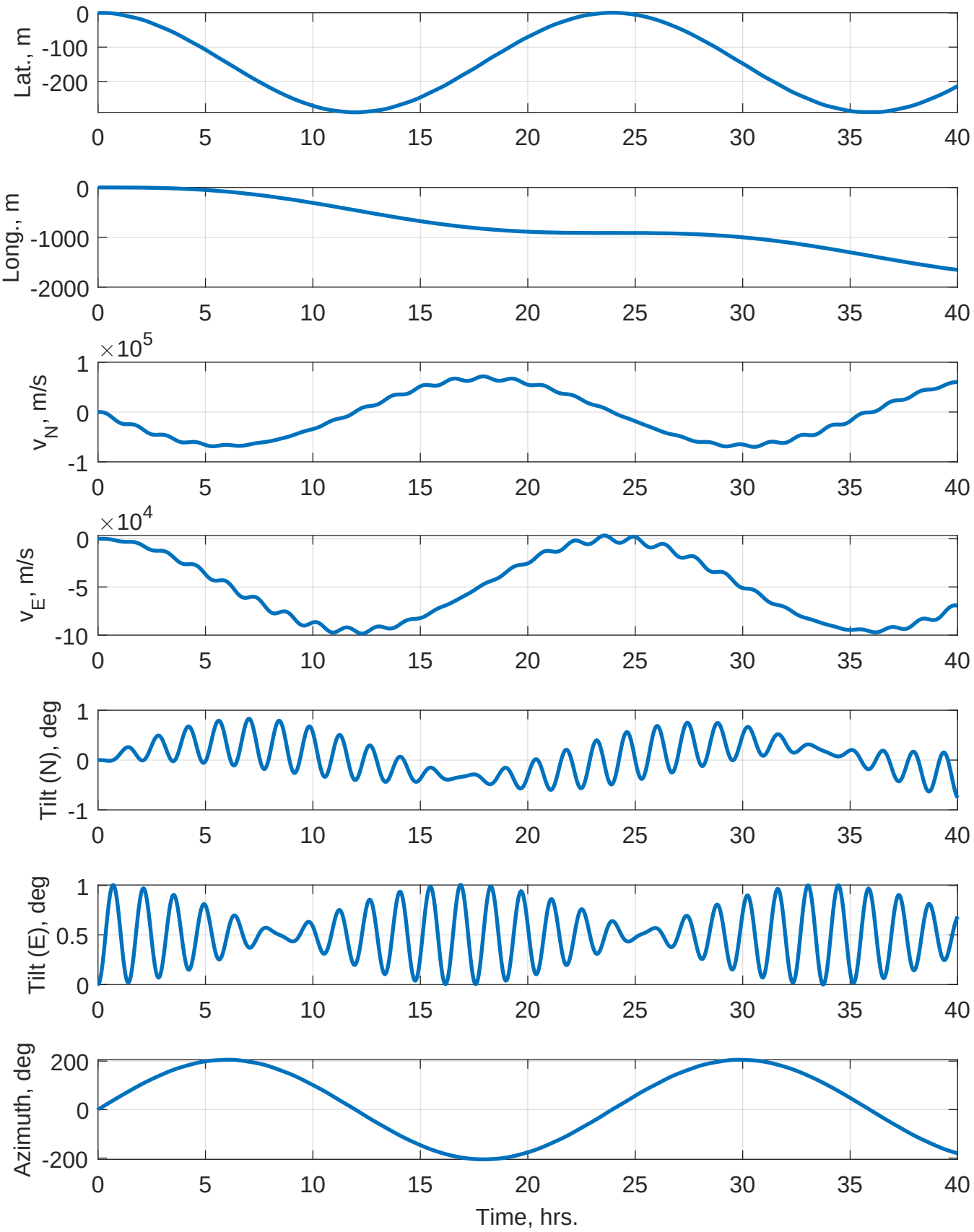

Fig.10 Stationary Force Response for 0.1 m/s^2 initial north accelerometer bias

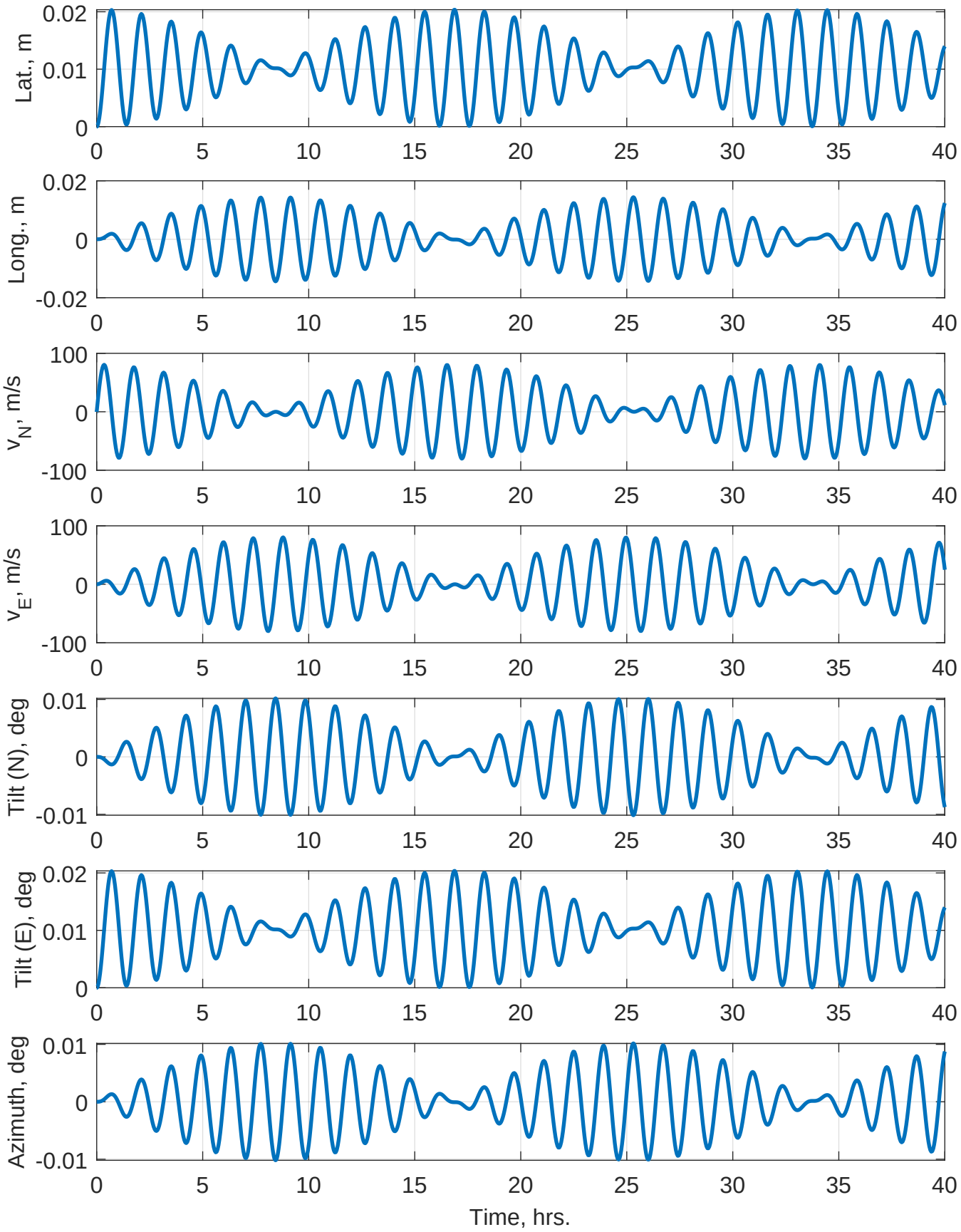

Fig.11 Stationary Force Response for 0.1 m/s^2 initial east accelerometer bias

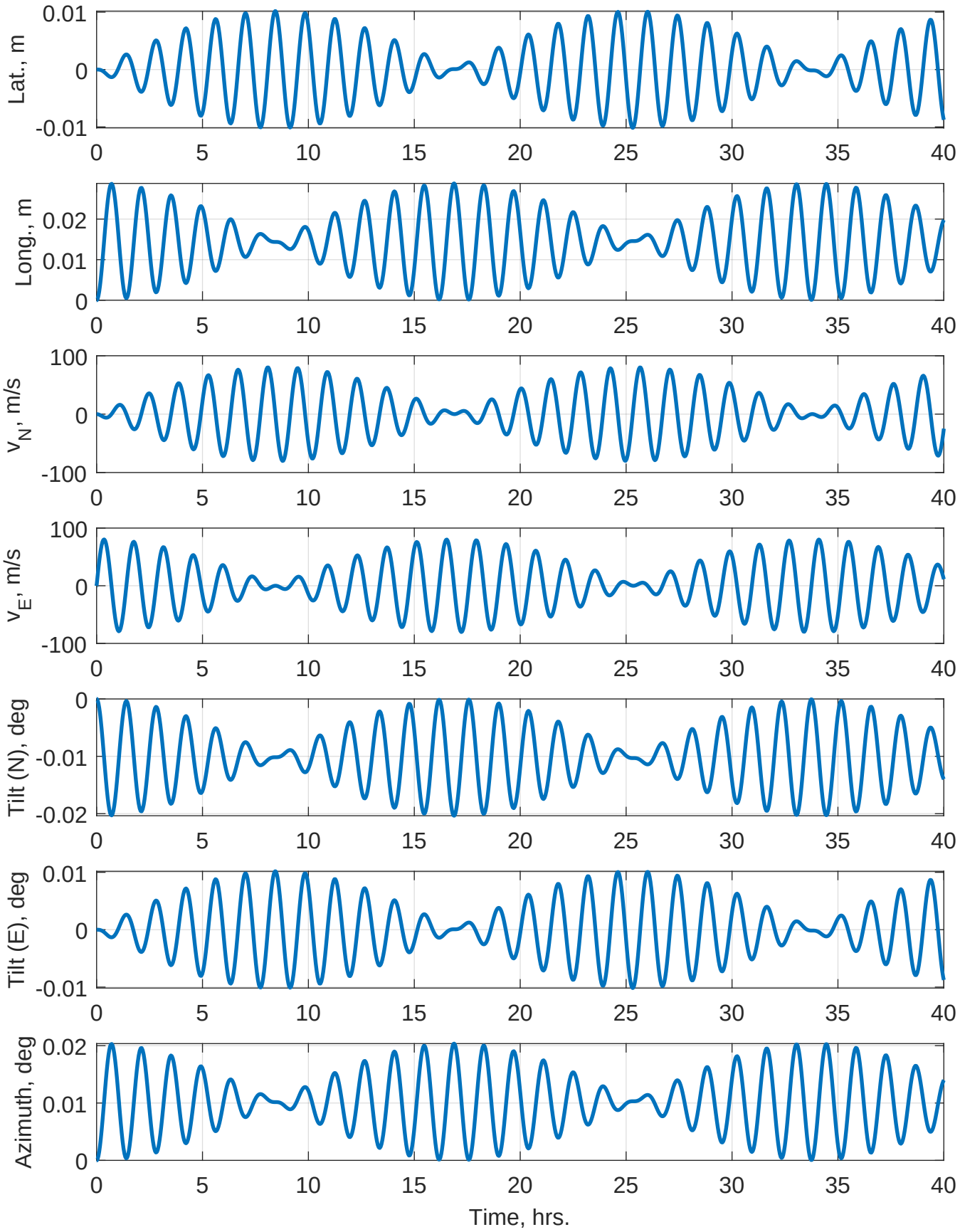

Chapter 4

Summary and Conclusion

In this project, the simulation study of linearized INS equation was performed. The nonlinear differential equations for INS were linearized by hand and verified with the references cited here in this report. It was observed from the study that the simulation results exhibits an oscillatory behavior for different sets of initial condition errors as expected with Foucault modulated Schuler oscillations. It is evident that any small error in provided initial condition to inertial navigator will result in significant but bounded errors over time. It is worth mentioning here that these errors do not grow unbounded because of feedback caused by earth's curvature surface. Foucault beats and Schuler oscillations were clearly observed in the simulation results. There were some assumption made during this work, i.e. radius of curvature is same for longitudinal and latitude direction, $R_\lambda = R_\phi = R_e$ and $\delta R_\phi = 0$, $\delta R_\lambda = 0$, along with some additional assumptions which can be found in [15]. It is important to study this dynamic error behavior and different error sources, so that methods to obtain accurate initial conditions such as alignment and gyro compassing can be developed. Further this simulation results serve as a reference to analysts for validating his algorithms. Apart from the course content, this project enabled the author to explore some topics which were not covered in detail and to develop understanding of initial condition error behavior in linearized INS differential equations. Overall it was a great learning experience for the author to study reference material and understand the basics of inertial navigation system as whole. References [15] and [16] were very useful resources for this project. The author is thankful to Prof. Demoz for his valuable guidance and advice during this project.

References

[1] Inertial Navigation Systems, Wikipedia Summary `https://en.wikipedia.org/wiki/Inertial_navigation_system`

[2] King, A. D. "Inertial navigation-forty years of evolution." GEC review 13, no. 3 (1998): 140-149.

[3] Widnall, W.S. and Grundy, P.A., 1973. Inertial navigation system error models. Intermetrics Incorporated.

[4] Kim, D., Shin, S. and Kweon, I.S., 2018. On-Line Initialization and Extrinsic Calibration of an Inertial Navigation System With a Relative Preintegration Method on Manifold. IEEE Transactions on Automation Science and Engineering, 15(3), pp.1272-1285.

[5] Schuler Oscillations, Paul G. Savage Strapdown Associates, Inc.

[6] Bar-Itzhack, I.Y. and Berman, N., 1988. Control theoretic approach to inertial navigation systems. Journal of Guidance, Control, and Dynamics, 11(3), pp.237-245.

[7] Benson, D.O., 1975. A comparison of two approaches to pure-inertial and Doppler-inertial error analysis. IEEE Transactions on Aerospace and Electronic Systems, (4), pp.447-455.

[8] Widnall, W.S. and Sinha, P.K., 1977. Comparison of Three Vertical Channel Designs for an Integrated GPS/Inertial Navigation System (No. IR-234). Intermetrics Inc. Cambridge MA.

[9] Miller, R.B., 1980. Strapdown inertial navigation systems: An algorithm for attitude and navigation computations (No. ARL/SYS-23). Aeronautical Research Labs Melbourne (Australia).

[10] Sciegienny, J., Nurse, R. and Wexler, J., 1976. Inertial Navigation System Standardized Software Development Final Technical Report Volume II of IV INS Survey and Analytical Development. Massachusetts, USA: Charles Stark Draper 1. aboratory, Inc.

[11] Agarwal, A., 2015. Sensor Fusion for Navigation of Autonomous Underwater Vehicle Using Kalman Filtering (Doctoral dissertation).

[12] Park, M. and Gao, Y., 2008. Error and performance analysis of MEMS-based inertial sensors with a low-cost GPS receiver. Sensors, 8(4), pp.2240-2261.

[13] Titterton, D., Weston, J.L. and Weston, J., 2004. Strapdown inertial navigation technology (Vol. 17). IET.

[14] Britting, K.R., 1971. Inertial navigation systems analysis.

[15] Farrell, J. and Barth, M., 1999. The global positioning system and inertial navigation (Vol. 61). New York: Mcgraw-hill.

[16] Farrell, J., 2008. Aided navigation: GPS with high rate sensors. McGraw-Hill, Inc..

[17] Groves, P.D., 2013. Principles of GNSS, inertial, and multisensor integrated navigation systems. Artech house.

[18] Rogers, R.M., 2007. Applied mathematics in integrated navigation systems. American Institute of Aeronautics and Astronautics.

[19] Hugon, P., 1964. Principles of Inertial Navigation for the Use of Air and Marine Vehicles and for Missiles. The International Hydrographic Review, 41(1).

[20] Kuritsky, M.M., Goldstein, M.S., Greenwood, I.A., Lerman, H., McCarthy, J.E., Shanahan, T., Silver, M. and Simpson, J.H., 1983. Inertial navigation. Proceedings of the IEEE, 71(10), pp.1156-1176.

[21] Linearizion Basics https://www.ece.rutgers.edu/ gajic/psfiles/linearization.pdf

Appendix A

MATLAB Simulation Code

- List of MATLAB Published Files

  1. `F.m`

     Linearized INS 15-State Error Equations Function Handle

  2. `main.m`

     Main Script that Integrates linearized INS Error Equations

Linearized INS 15-State Error Equations

```
function dxdot = F(t,dx) %#ok<INUSL>
%
 ========================================================================
% This function represents the 15-State linearized INS state error
 equation
%
% Linearized States (dx) in NED (North-East-Down) Navigation frame are
% defined as below.
%
% Position Errors dP    = [del_lat; del_long; ; del_alt];
%                       = [dphi; dlambda; dh];
%
% Velocity Errors dVn   = [del_vN; del_vE; del_vD];
%                       = [dvN; dvE; dvD];
%
% Attitude Errors dPSIn = [del_psiN; del_psiE; del_psiD];
%                       = [dpN; dpE; dpD];
%
% NOTE: RHO = [psiN; psiE; psiD] are positively defined small-angle
% rotations about the navigation-frame axis to align the navigation
 frame
% with the computed navigation-frame. epsN and epsD are referred to as
 tilt
% errors and epsD is referred to as the heading, yaw or azimuth error.
%
% Additional Forcing (6-States) Can be provided by Accelerometer
 Errors
% (dae) Gyro Errors (dge)
%
% References:
% [1] W. S. Widnall and P. A. Grundy, Inertial Navigation System Error
% Models, Technical Report TR-03-73, Intermetrics, Cambridge, MA,
 1973.
%
% [2] Farrell, J. and Barth, M., 1999. The global positioning system
 and
% inertial navigation (Vol. 61). New York: Mcgraw-hill.
%
 ========================================================================

% Author: Jyot R. Buch
% Ph.D. Student in Aerospace Engineering and Mechanics
% University of Minnesota, Twin Cities
% Copyright (c) 2019, All Rights Reserved.
% Course Project : Navigation and Attitude Determination Systems

% Vehicle is nominally located at 45 deg North Latitude and 45 deg
 East
% Longitude and sea-level i.e. h = 0 Altitude
phi = deg2rad(45);
```

```
h = 0;

% Earth Radii of curvature
[Rphi,Rlambda] = earthrad(phi);
Re = sqrt(Rlambda*Rphi); % m

% Gravity Model
g = norm(glocal(phi,h));

% Earth Rate
omega_n_ie = earthrate(phi);
omega_ie = norm(omega_n_ie); % rad/sec

% Stationary Error Analysis
fE = 0;
fN = 0;
fD = -g;
vD = 0;
vN = 0;
vE = 0;

% Table 6.1 [2]
OMEGAN = omega_ie * cos(phi);
OMEGAD = -omega_ie * sin(phi);
rhoN = vE/Re;
rhoE = -vN/Re;
rhoD = -vE*tan(phi)/Re;
omegaN = OMEGAN + rhoN;
omegaE = rhoE;
omegaD = OMEGAD + rhoD;

% Table 6.2 [2]
kD = vD/Re;
F41 = -2*OMEGAN*vE - rhoN*vE/(cos(phi)^2);
F43 = rhoE*kD - rhoN*rhoD;
F51 = 2*(OMEGAN*vN + OMEGAD*vD) + rhoN*vN/(cos(phi)^2);
F53 = -rhoE*rhoD - kD*rhoN;
F55 = kD - rhoE*tan(phi);
F63 = rhoN^2+rhoE^2 - (2*g/Re);

% F terms
F13 = rhoE/Re;
F14 = 1/Re;
F21 = -rhoD/cos(phi);
F23 = -rhoN/(Re*cos(phi));
F25 = 1/(Re*cos(phi));
F36 = -1;
F44 = kD;
F45 = 2*omegaD;
F46 = -rhoE;
F48 = fD;
F49 = -fE;
F54 = -(omegaD+OMEGAD);
F56 = omegaN + OMEGAN;
```

```
F57 = -fD;
F59 = fN;
F61 = -2*vE*OMEGAD;
F64 = 2*rhoE;
F65 = -2*omegaN;
F67 = fE;
F68 = -fN;
F71 = -OMEGAD;
F73 = rhoN/Re;
F75 = -1/Re;
F78 = omegaD;
F79 = -omegaE;
F83 = rhoE/Re;
F84 = 1/Re;
F87 = -omegaD;
F89 = omegaN;
F91 = OMEGAN + (rhoN/(cos(phi)^2));
F93 = rhoD/Re;
F95 = tan(phi)/Re;
F97 = omegaE;
F98 = -omegaN;

% dxdot = F(t)*dx(t) + f(t);
F = [...
    0   0   F13 F14 0   0   0   0   0   ;
    F21 0   F23 0   F25 0   0   0   0   ;
    0   0   0   0   0   F36 0   0   0   ;
    F41 0   F43 F44 F45 F46 0   F48 F49 ;
    F51 0   F53 F54 F55 F56 F57 0   F59 ;
    F61 0   F63 F64 F65 0   F67 F68 0   ;
    F71 0   F73 0   F75 0   0   F78 F79 ;
    0   0   F83 F84 0   0   F87 0   F89 ;
    F91 0   F93 0   F95 0   F97 F98 0   ;...
    ];

% Remove 3rd and 6th row and column because vertical dynamics are
 unstable
% They will cause other states to blow up and oscillations will not be
% observed. First remove 6th and then 3rd so no ambiguity in matrix
% indexes.
F(6,:) = [];
F(:,6) = [];
F(3,:) = [];
F(:,3) = [];

% Extract gyro and Accelerometer error States
dae = dx(10:12);
dge = dx(13:15);

% 7 states
derrors = [0;0;dae(1:2);dge];
dx = [dx(1:2); dx(4:5); dx(7:9)];

% Return forced dxdot, i.e. with gyro and Accelerometer bias
```

```
% Accelerometer Errors affect accelration equation i.e. velocity
 components
% Rate Gyro Errors affect small-angle rotations
dxdot = F*dx + derrors;
dxdot = [dxdot(1:2); 0; dxdot(3:4); 0; dxdot(5:7); zeros(6,1)];
end
```

Published with MATLAB® R2018b

Main Script

Table of Contents

Integrate Linearized INS Error Equations

Prepare Workspace

```
clear;close all;clc;addpath('./gnss_ins_functions/');
```

Simulation Parameters

```
% ODE45 Params
T0 = 0;
Tf = 40*3600; % 40 h
tspan = [T0 Tf];

% Vehicle is nominally located at 45 deg North Latitude and 45 deg
 East
% Longitude and sea-level i.e. h = 0 Altitude
phi = deg2rad(45);
lambda = deg2rad(45);
h = 0;

% Earth Radii of curvature
[Rphi,Rlambda] = earthrad(phi);
Re = sqrt(Rlambda*Rphi); % m

% Gravity Model
g = norm(glocal(phi,h));

% Earth Rate
omega_n_ie = earthrate(phi);
omega_ie = norm(omega_n_ie); % rad/sec

% Schuler Frequency
ws = sqrt(g/Re);TSchuler = (2*pi)/ws;
fprintf('Schuler Period : %4.3f min\n',TSchuler/60);

% Foucalt Frequency
wf = omega_ie*sin(lambda);TFoucalt = (2*pi)/wf;
fprintf('Foucalt Period : %4.3f h\n',TFoucalt/3600);
```

```
Schuler Period : 84.455 min
```

Foucalt Period : 33.848 h

Stationary Error Response

```
% Linearized 15-States [dP; dV; dPSIn; dae; dge;]
% i.e. [dPosition; dVelocity; dAttitude; dAccelerometerBias;
 dGyroBias;]
x0 = {...
    [1000; 0; 0; 0; 0; 0; 0; 0; 0; 0; 0; 0; 0; 0; 0;],...
    [0   ; 0; 0; 1; 0; 0; 0; 0; 0; 0; 0; 0; 0; 0; 0;],...
    [0   ; 0; 0; 0; 1; 0; 0; 0; 0; 0; 0; 0; 0; 0; 0;],...
    [0   ; 0; 0; 0; 0; 0; 1; 0; 0; 0; 0; 0; 0; 0; 0;],...
    [0   ; 0; 0; 0; 0; 0; 0; 1; 0; 0; 0; 0; 0; 0; 0;],...
    [0   ; 0; 0; 0; 0; 0; 0; 0; 1; 0; 0; 0; 0; 0; 0;],...
    };
sgtitleArray = {...
    'Stationary Error Response for 1 km initial longitude error',...
    'Stationary Error Response for 1 m/s initial north velocity
 error',...
    'Stationary Error Response for 1 m/s initial east velocity
 error',...
    'Stationary Error Response for 1 deg initial north tilt error',...
    'Stationary Error Response for 1 deg initial east tilt error',...
    'Stationary Error Response for 1 deg initial azimuth tilt
 error',...
    };

% Numerical Integration
for j = 1:length(x0)
    % ODE45
    [t,dx] = ode45(@F,tspan,x0{j});

    % Plot
    figure;k = 1;
    ylabelArray = {'Long., m','Lat., m','v_N, m/s','v_E, m/s',...
        'Tilt (N), deg','Tilt (E), deg','Azimuth, deg'};
    for i = [1,2,4,5,7,8,9]
        subplot(7,1,k);
        plot(t/3600,dx(:,i));ylabel(ylabelArray{k});k = k + 1;
    end
    xlabel('Time, hrs.');sgtitle(sgtitleArray{j});pp;
    print(gcf,'-dpdf',sprintf('unforced_fig%d',j),'-fillpage');
end
```

Stationary Forced Response [Including Accelerometer and Gyro Errors]

```
% Linearized 15-States [dP; dV; dPSIn; dae; dge;]
% i.e. [dPosition; dVelocity; dAttitude; dAccelerometerBias;
 dGyroBias;]
x0 = {...
```

```
    [0; 0; 0; 0; 0; 0; 0; 0; 0; 0;   0;   0; 0.015; 0;     0;     ],...
    [0; 0; 0; 0; 0; 0; 0; 0; 0; 0;   0;   0; 0;     0.015; 0;     ],...
    [0; 0; 0; 0; 0; 0; 0; 0; 0; 0;   0;   0; 0;     0;     0.015;],...
    [0; 0; 0; 0; 0; 0; 0; 0; 0; 0.1; 0;   0; 0;     0;     0;     ],...
    [0; 0; 0; 0; 0; 0; 0; 0; 0; 0;   0.1; 0; 0;     0;     0;     ],...
    };
sgtitleArray = {...
    'Stationary Force Response for 0.015 deg/h initial north gyro
 bias',...
    'Stationary Force Response for 0.015 deg/h initial east gyro
 bias',...
    'Stationary Force Response for 0.015 deg/h initial azimuth gyro
 bias',...
    'Stationary Force Response for 0.1 m/s^2 initial north
 accelerometer bias',...
    'Stationary Force Response for 0.1 m/s^2 initial east
 accelerometer bias',...
    };

% Numerical Integration
for j = 1:length(x0)
    % ODE45
    [t,dx] = ode45(@F,tspan,x0{j});

    % Plot
    figure;k = 1;
    ylabelArray = {'Long., m','Lat., m','v_N, m/s','v_E, m/s',...
        'Tilt (N), deg','Tilt (E), deg','Azimuth, deg'};
    for i = [1,2,4,5,7,8,9]
        subplot(7,1,k);
        plot(t/3600,dx(:,i));ylabel(ylabelArray{k});k = k + 1;
    end
    xlabel('Time, hrs.');sgtitle(sgtitleArray{j});pp;
    print(gcf,'-dpdf',sprintf('forced_fig%d',j),'-fillpage');
end
```

Cleanup Workspace

```
rmpath('./gnss_ins_functions/');
```

Published with MATLAB® R2018b